

The Discharge Pressure and Longitudinal Magnetic Field Dependence of Plasma Parameters via Optical Emission Spectroscopy at the Magnetron Sputtering System

Waleed I. Yaseen¹, Mohammed K. Khalaf², Dawood S. Ali³

¹Dept. of Astronomy and Space, College of Science, University of Baghdad

²Center of Applied Physics, Baghdad, Iraq

³Dept. of Physics, College of Education for Pure Sciences University of Anbar

Abstract: *In this work, plasma parameters can be accurately calculated when the intensities of two spectral lines are experimentally known. The magnetic field effect on the plasma parameters and the intensity spectrum for glow discharge in argon at low pressures has been investigated by using optical emission spectroscopy technique. The longitudinal magnetron system used in this work, where the open field unbalanced magnetron was employed at the cathode and anode electrode. The plasma parameters have been studied in presence of magnetic field of 855 Gauss and argon gas pressure ranges from (0.25 to 0.85) mbar. Applying a longitudinal magnetic field yields confining the plasma near discharge electrodes. This confining corresponds to the maximum enhancement of the spectral lines intensity (ArI 750.3nm and ArII 434.7nm) and the electron density is a maximum. In the presence of the magnetic field, the values of the electron temperature T_e are smaller than that without magnetic field. An increase in gas pressure, resulting in a slight decrease of plasma density at low gas pressure (0.33 mbar) but it increased at higher gas pressure. Also, results show that the electron temperature drops slowly as pressure is increased from (0.25 to 0.5) mbar, but it drops rapidly at higher pressures of 0.85 mbar and the maximum values of this parameter are obtained at 0.33 mbar pressure.*

Keyword: DC discharge, plasma parameters, optical emission spectroscopy, longitudinal magnetic field, ion sputtering

1. Introduction

Radio-frequency (rf) plasma is widely used as a low temperature plasma processing medium for material processing in many fields including microelectronics, aerospace, and the biology [1, 2]. As a result of energetic ions, chemically active species, radicals and also energetic neutral species, rf discharges are widely used in etching, deposition and surface treatment, particularly in the semiconductor industry. Although, much processing is done on an empirical basis for a particular device, a full characterization is desirable for reproducibility, consistency, better understanding the process, and more importantly transformation of process from one device to another [3,4]. The Penning Discharge was a first step towards the construction of a magnetron [5]. The development of high performance magnetron sputtering sources allowed sputtering to be performed at higher deposition rates [6], and can be used for high-purity thin film fabrication in semiconductors or for large-area coatings of structural materials such as the glass windows. One of the main advantages of magnetron sputtering over the other competing physical vapor deposition techniques is the additional kinetic energy of the sputtered atoms. This kinetic energy can lead to a more adherent coating and better conformal coverage. It also benefits the formation of many different compound thin films at much lower temperature, which is a great advantage when the temperature-sensitive substrates are used [7, 8]. Magnetron sputtering is somewhat different from general sputtering technology. The difference is that magnetron sputtering technology uses magnetic fields

to keep the plasma in front of the target, intensifying the bombardment of ions. Highly dense plasma is the result of this PVD coating technology. Nowadays, Magnetically-sputtered dc discharges as magnetron sputtering systems are widely used for depositing the nanostructures thin films and high temperature superconducting materials [9-11]. Magnetron sputtering allows charged particle bombardments can have a large effect on deposition efficiency and quality of the sputtered films by changing the magnetron configuration. Electrons and ions with high energy bombarding the film change the nucleation characteristics, the mobility of sputtered particles on the substrate and the crystallographic structure of the film [12]. Before applying the plasma discharges for any purpose, it is necessary to determine the basic discharge parameters like electron temperature and plasma density and to understand their dependence on the discharge parameters such as discharge voltage and operating gas pressure. Various methods, such as emission or absorption optical spectroscopy, microwave interference, mass spectroscopy and Langmuir probe have been used to diagnose the plasma. Optical methods such as emission, absorption, laser scattering, or fluorescence spectrometry are proven techniques for probing various parts of the plasma without disturbing its state and composition [13]. Among these techniques, there is the optical emission spectroscopy. This technique is based on the measurement of the optical radiation emitted from the plasma as it reflects the properties of the plasma in the immediate environment of atomic, molecular, and ionic radiators. Radiation is a result of the electron or ion interaction with other molecules in the plasma. Four plasma models were suggested by MC

Volume 7 Issue 1, January 2018

www.ijsr.net

Licensed Under Creative Commons Attribution CC BY

Whiter criterion which is dependent on the mechanism of electron interaction. Three methods are available for electron temperature measurement, these are [13,14]:

- 1) The ratio of two lines' intensity;
- 2) The ratio of a line to continuum intensity;
- 3) The ratio of two parts of continuum intensities.

The first method will be used in this paper for the estimation of the mean electron temperature in the argon DC glow discharge. The intensity of these spectral lines depends on (kT_e) , and always proportional to the population density of excited states. Hence, (kT_e) can be determined using these spectral line intensities and well-know Boltzmann plot [15]:

$$kT_e = (E_2 - E_1) \left[\ln \frac{I_1 \lambda_1 g_2 A_2}{I_2 \lambda_2 g_1 A_1} \right]^{-1} \quad (1)$$

The indices 1 and 2 refers to the first and second spectral lines, I is the intensity, k is the Boltzmann constant, g is the statistical weight, E is the excited state's energy and A is the transition probability. The Boltzmann plot method is only valid if the discharge plasma under study is in complete local thermodynamic equilibrium (LTE). In this spectrum, the argon emitted lines are observed in the range of 200-900 nm and kT_e is determined by selecting two Ar-I spectral lines. In calibration, the E, g and A for selected lines is taken from the National Institute of Standards and Technology NIST Atomic Spectra Datasheet [16,17]. The n_e can be determined using the relative intensities of atomic and ionic spectral lines in Boltzmann -Saha equation [15].

$$n_e = \left[\frac{(2\pi m k T_e)^{3/2}}{h^3} \right] \left[\frac{2A_2 g_2 \lambda_1 I_1}{A_1 g_1 \lambda_2 I_2} \right] e^{\left[\frac{-(E_2 - E_1 + E_1 - \Delta E)}{kT_e} \right]} \quad (2)$$

Where, (1, 2) denote the neutral and ionized atoms, E is the energy of the emissive levels, E_i is the ionization energy of the neutral atoms and ΔE is the lowering of ionization energy [14, 15].

2. Experimental Setup

Fig.(1) shows a schematic diagram of the main parts of the longitudinal magnetron system used in this work, where the open field unbalanced magnetron was employed at the cathode and anode electrode. Magnetic field strength is equal to 855 G. The belljar vacuum chamber made of glass, was used with length 35 cm and diameter 14.5 cm. Electrodes were made of stainless steel and each was a disk of 7.25 (cm) in diameter and 4 mm in thickness. Two annular concentric magnets were placed behind each electrode to form the magnetron configuration. The outer diameters 6 cm and magnet diameter from the inside is 2.5 cm. The electrodes were connected to a DC power supply to provide the electrical power required for discharge. The lower electrode (anode) could move vertically with respect to the fixed upper electrode (cathode). Pure argon gas was used to produce the discharge plasma. A DC power supply (up to 3 kV and 100mA) was used for electrical discharge between the electrodes and breakdown voltages and discharge current were monitored by digital voltmeter and ammeter, respectively. A current limiting resistor of 6.8 k Ω was connected in series to the discharge circuit in order to control the current flowing in the circuit. The discharge chamber was evacuated by a two stage (16 m³/h) Leybold Hearers rotary pump and the vacuum inside the chamber was measured by pirani gauge connected to a vacuum controller from China -ZDZ-52. Argon gas was supplied to the chamber through a fine-controlled needle valve (0 - 100 sccm) to control the gas pressure inside the chamber. Spectrum measurements were obtained by using the spectrometer of spectrum VS2100, optical fiber and collimating lens as showing Fig.(1)

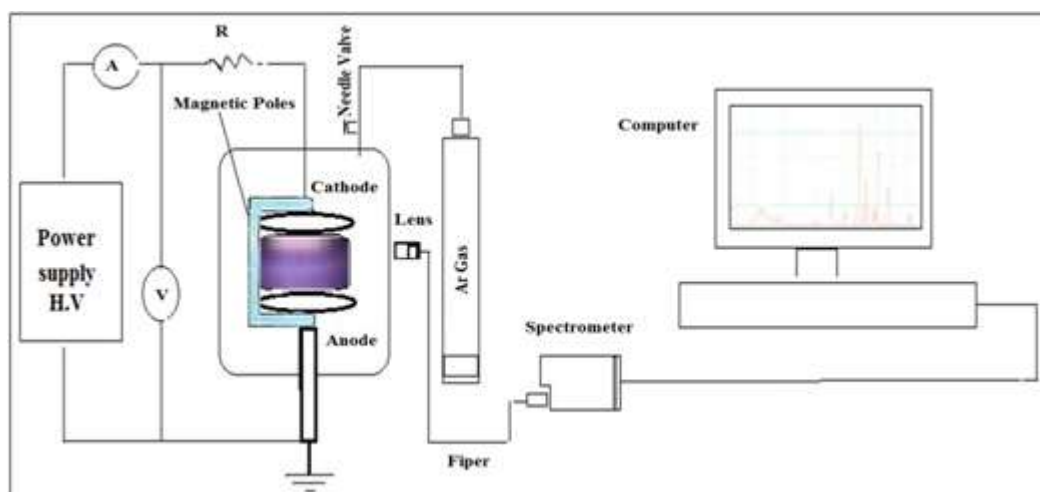


Figure 1: The schematic diagram of longitudinal magnetron system

3. Results and Discussion

The emission spectra of the plasma argon produced between electrodes at pressure from 0.5 to 0.8mbar, with and without magnetic field are shown in Figures 2 and 3. The intensity of the lines increases by increasing the gas pressure, where the intensity of the lines has been found to be proportional to p^α ,

where α is constant, which varies between 0.2–0.5, depending on the wavelength [14]. Figs. (4 and 5) represent the intensity of 750.3 nm lines and 434.7 nm lines respectively as a function of the gas pressure in DC power with and without magnetic field, where intensity increases by increasing gas pressure (p) and the intensity increases with magnetic field in two lines. Two suitable lines, one for

ArI and other one for ArII are chosen and an electron temperature is estimated using the lines intensity ratio method. Considering Ar I line of wavelength 750.3 nm and ArII line with wavelength 434.7 nm by using NIST we get:

ArI (750.3 nm), $A_1 = 4.45 \times 10^7 \text{ S}^{-1}$, $g_1 = 3$, $E_1 = 11.828 \text{ eV}$
 ArII (434.7 nm), $A_2 = 1.17 \times 10^8 \text{ S}^{-1}$, $g_2 = 6$, $E_2 = 16.643 \text{ eV}$
 For the measurement of electron temperature use Eq. (1).

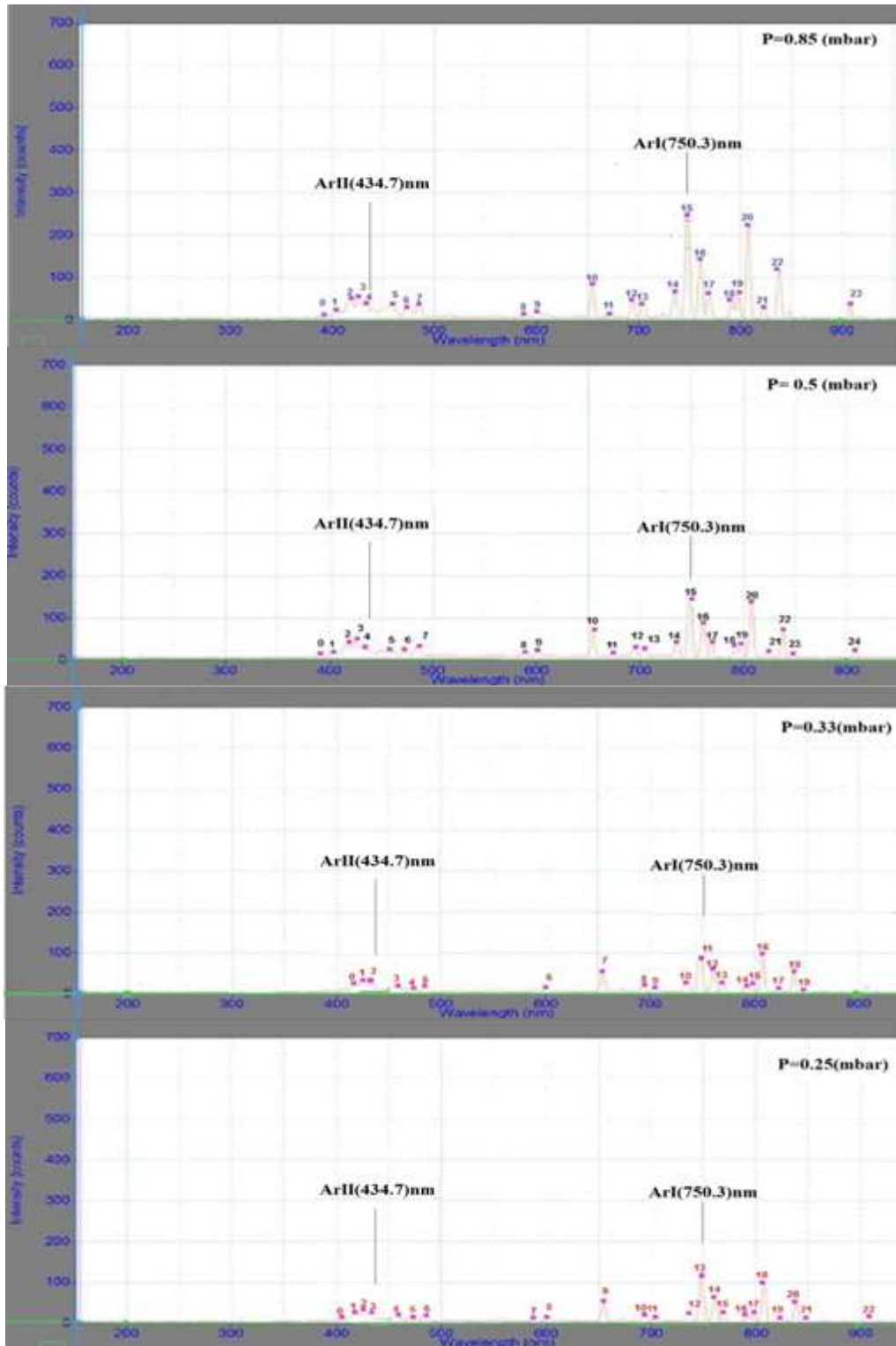


Figure 2: The emission spectra for plasma argon at different pressures without magnetic field.

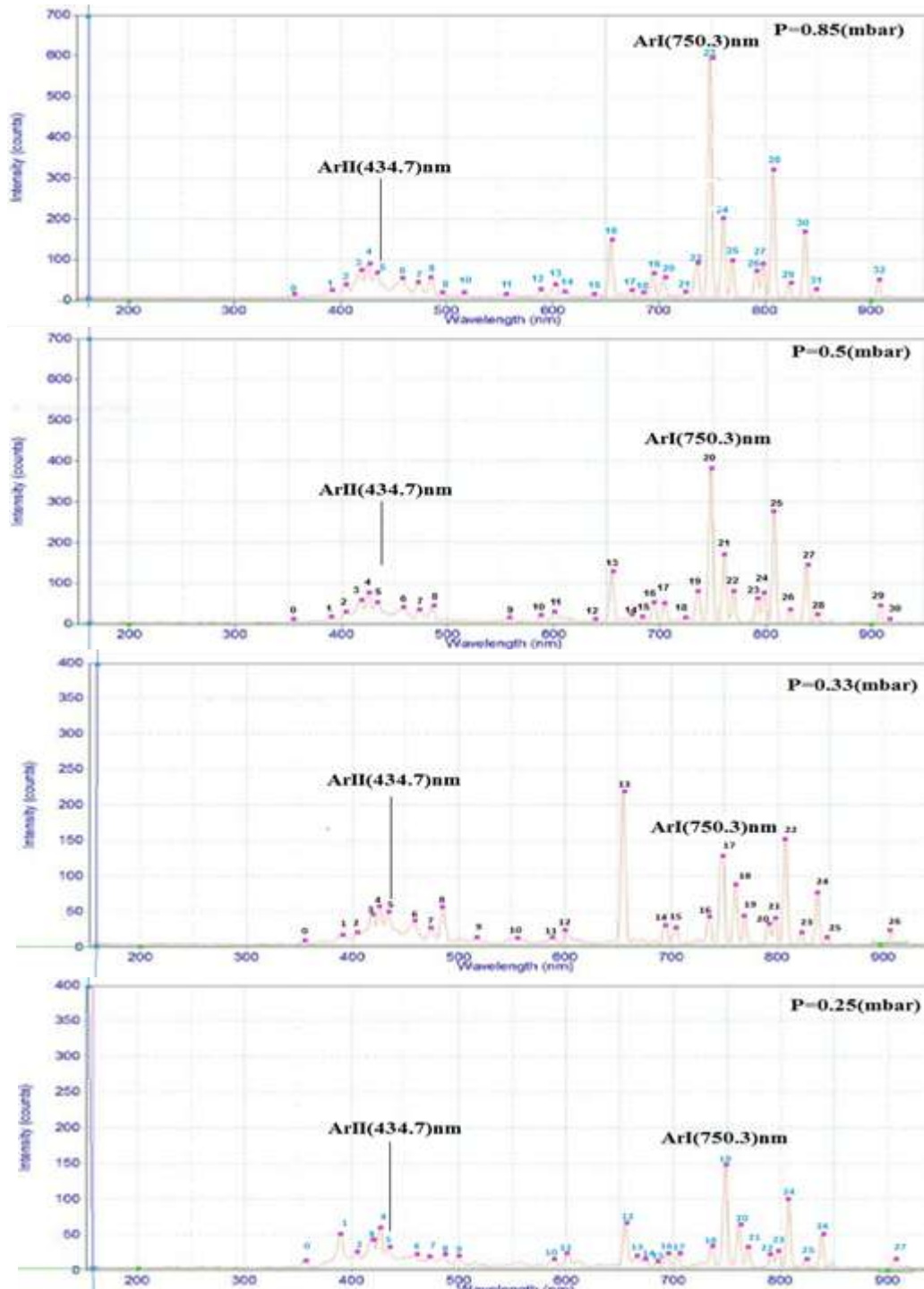


Figure 3: The emission spectra for plasma argon at different pressures with magnetic field

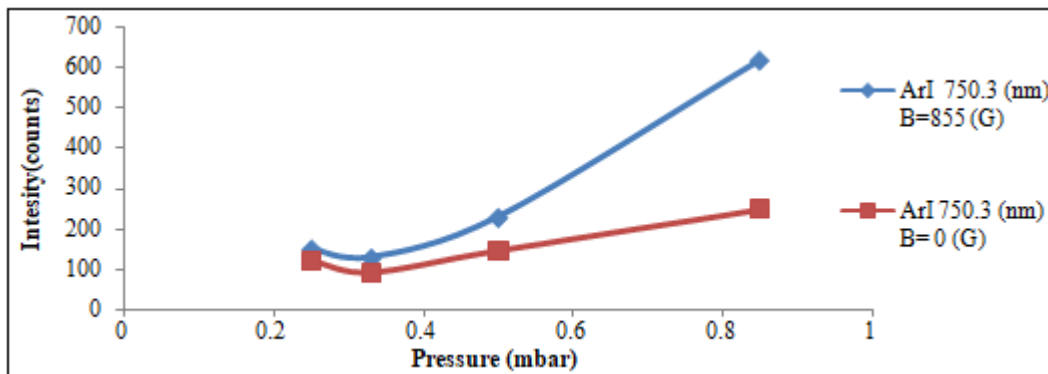


Figure 4: Intensity of 750.3 nm line varying with pressure with and without magnetic field.

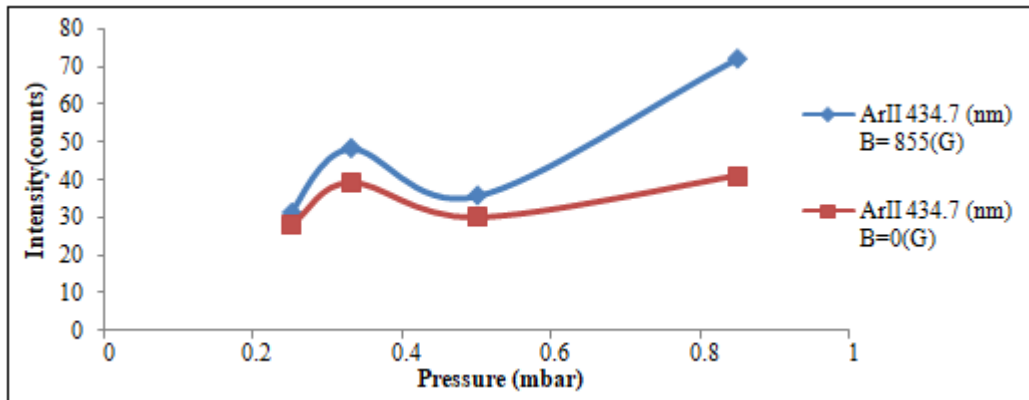


Figure 5: Intensity of 434.7 nm line varying with pressure with and without magnetic field.

The effect of the argon pressure on the electron temperature with and without magnetic field is shown in Fig. (6). It is obvious that the electron temperature drops slowly as pressure is increased from (0.25- 0.5) mbar, but is relatively drops rapidly at higher pressures 0.85 mbar. At higher pressures there is a greater energy transfer between the electrons and the surrounding argon atoms. The electron temperature drop may be due to the decreased of the drift velocity of the electrons with increasing of collisions with increasing gas atoms density. On other hand, the electron temperature curve is shifted to down at using magnetic field. It could be explained as follows: the presence of longitudinal magnetic field will cause the electrons to move with helical path which increases the probability of collision with atoms and ions; this will reduce the effective free path and hence decreasing the kinetic energy of the electrons and electron temperature [17].

It is obvious from eq. (2) that there is inverse relation between electron temperature and electron density so

decrease in electron temperature means to increase the electron density. Figure 7 shows the dependence of plasma density on argon pressure. By the increase of the gas pressure, the plasma density decreased slightly at low gas pressure (0.33 mbar) while it increased at higher gas pressure. The variation of electron density in Fig.7 shows a linear increment of density with pressure, which is obvious due to the increment of collisions with increasing pressure. The parameters T_e and n_e are obtained from OES and the pressure dependence comparison with other results [18] generally shows good agreement. As longitudinal magnetic field is used the electron density increases compared without magnetic field. The electrons moving through a longitudinal magnetic field have helical paths around longitudinal magnetic field thus it may gain enough acceleration to ionize gas atoms leading to increasing electron density by inelastic collision with another particle (ion and atom argon) [10].

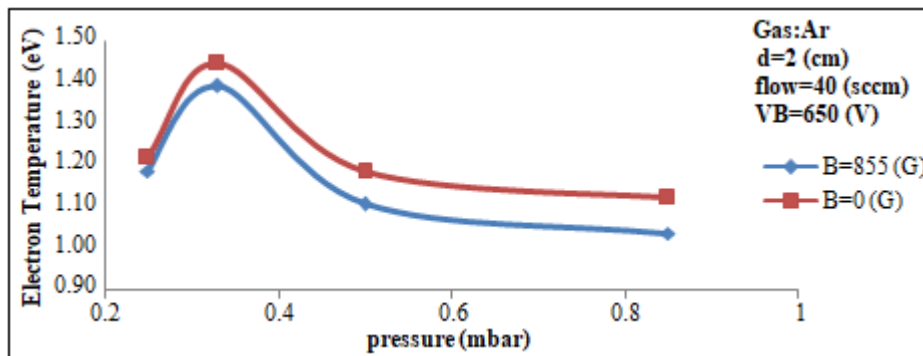


Figure 6: Variation of the electron temperature (T_e) with the pressure with and without magnetic field.

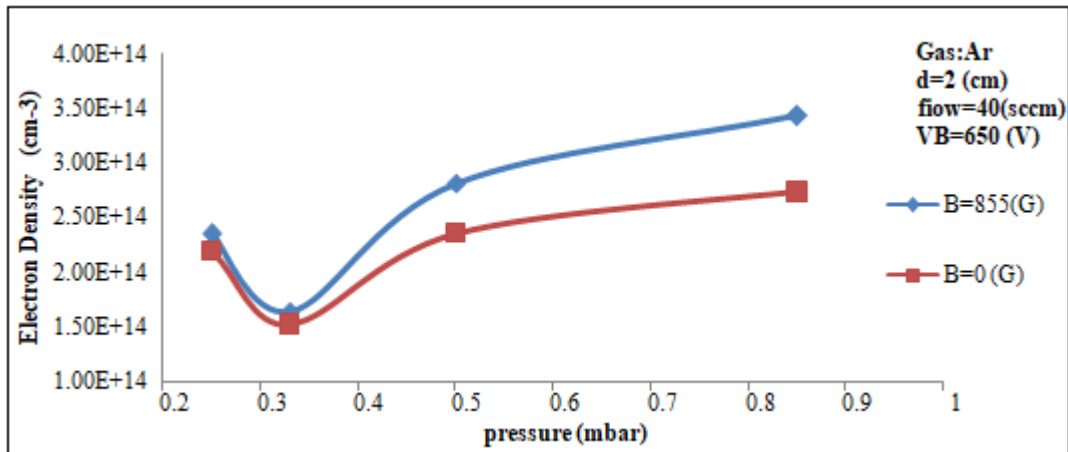


Figure 7: Variation of the electron density (n_e) with the pressure with and without magnetic field.

4. Conclusions

We studied the pressure dependence of characteristic plasma parameters in longitudinal magnetron system. The optical emission spectroscopy method is used to characterize the low pressure DC glow discharge. A magnetic field and working gas pressure dependent increase in lines intensity, which presents at $\sim 855\text{G}$, is observed at gas pressure up to 0.2mbar . It is found that electron temperature gradually decreases with the increase in working pressure while electron density increases at low gas pressure. Similar trends also have been observed in case of electron temperature and density in presence of longitudinal magnetic fields

References

- [1] K. H. Becker, U. Kogelschatz, K. H. Schoenbach, R. J. Barker, "Non-Equilibrium Air Plasmas at Atmospheric Pressure", Institute of Physics Publishing, Bristol, Philadelphia, 2005.
- [2] E. Valderrama, M. Favre, H. Bhuyan, H.M. Ruiz, E. Wyndham, J. Valenzuela, H. Chuaqui, "Sub-micron size carbon structures synthesized using plasma enhanced CVD, without external heating and no catalyzer action", Surface & Coatings Technology, vol. 204, pp. 2940–2943, (2010).
- [3] A. Dyson, P. Bryant and J. E. Allen, "Multiple harmonic compensation of Langmuir probes in rf discharges", Meas. Sci. Technol., vol. 11, pp. 554-559, (2000).
- [4] H. Biederman, P. Bílková, J. Ježek, P. Hlídek, D. Slavínská, "RF magnetron sputtering of polymer", J. Non-Crystalline Solids Vol. 218, pp. 44-49, (1997).
- [5] E. Nasser, "Fundamentals of gaseous ionization and plasma electronics", John Wiley & Sons, Inc. (1971).
- [6] J.A Thornton, J.E Greene, "Sputter deposition processes, in Handbook of Deposition Technologies for Films and Coatings", pp. 275-337, Ed. (1994).
- [7] S. Berg and T. Nyberg, "Fundamental understanding and modeling of reactive sputtering processes", Thin Solid Films, 476, 215, (2005).
- [8] N. Li, J. P. Allain, and D. N. Ruzic, "Enhancement of aluminum oxide physical vapor deposition with secondary plasma", Surf. Coat. Technol., 149, 161, (2002).
- [9] G. Lengl, P. Ziemann, F. Banhart, and P. Walther, "Anomalous behavior of gold nanoislands on top of SrTiO₃ (0 0 1) during their overgrowth by thin YBaCuO films", Sci. Direct, vol. 390, pp. 175–184, (2003).
- [10] O. Bilyk, A. Marek, P. Kudrna, J. F. Behnke, and M. Tich, "2-D Experimental Study of the Plasma Parameter Variations of the Magnetically Sustained DC Discharge in Cylindrical Symmetry in Argon", Contrib. Plasma Phys. 44, no. 7-8, pp. 613–618, (2004).
- [11] A. S. Hasaani, "Magnetic Field Effect on the Characteristics of Large-Volume Glow Discharge in Argon at Low Pressure", Iraqi J. Sci., vol. 57, no. 1, pp. 135–144, (2016).
- [12] J. Veldeman, H. Jia, and M. Burgelman, "Influence of magnetron configuration on CoCr films sputtered on flexible substrates", Journal of Magnetism and Magnetic Materials, Vol. 193, no.1-3, p. 128-131, (1999).
- [13] A. A. Garamoon, A. Samir, F. F. Elakshar, A. Nosair, and E. F. Kotp, "Spectroscopic study of Argon DC glow discharge", IEEE Trans. Plasma Sci., vol. 35, no. 1, pp. 1–6, (2007).
- [14] F. U. Khan, N. U. Rehman, S. Naseer, M. A. Naveed, A. Qayyum, N. A. D. Khattak, and M. Zakaullah, "Diagnostic of 13.56 MHz RF sustained Ar – N₂ plasma by optical", Eur. Phys. J. Appl. Phys., vol. 45, 11002, (2009).
- [15] M. Y. Naz, A. Ghaffar, N. U. Rehman, S. A. Shahid, and S. Shukrullah, "Characterization of an In-house Built 50 Hz Single Dielectric Barrier Discharge System Having Asymmetric Electrodes", Int. J. Eng. Technol. IJET-IJENS Vol.12 no. 5, (2012).
- [16] A. Kramida, Ralchenko, Yu., Reader, J, "NIST Atomic Spectra Database (Ver. 5.1)", in, National Institute of Standards and Technology, Gaithersburg, MD. [Gaithersburg, Md.], (2013).
- [17] F. M. Jasim, "Effect of axial magnetic field on DC glow discharge plasma parameters in nitrogen at moderate pressure", M.Sc. thesis, University of Mosul. (2005).
- [18] M. Sakaki, T. Sakakibara, "Pressure dependence of plasma parameters in medium-vacuum nitrogen arc discharge with the titanium cathode" IEEE Transactions on Plasma Science, Vol.19, 1, (1991)